Kinetics and Catalysis, Vol. 46, No. 2, 2005, pp. 189–203. Translated from Kinetika i Kataliz, Vol. 46, No. 2, 2005, pp. 203–218.

TiO_2 Photocatalytic Oxidation: I. Photocatalysts for Liquid-Phase and Gas-Phase Processes and the Photocatalytic Degradation of Chemical Warfare Agent Simulants in a Liquid Phase

A. V. Vorontsov*, D. V. Kozlov*, P. G. Smirniotis, and V. N. Parmon***

** Boreskov Institute of Catalysis, Siberian Division, Russian Academy of Sciences, Novosibirsk, 630090 Russia*

*** University of Cincinnati, Cincinnati, OH 45221-0012, USA*

Received April 1, 2004

Abstract—The results of studies on the effect of the preparation procedure on the properties of TiO_2-based photocatalysts and the kinetics and mechanism of the photocatalytic oxidation of organic water pollutants are surveyed. The effects of calcination temperature, surface modification with platinum, and acid–base treatment of the surface of titanium dioxide on its activity in model gas-phase and liquid-phase reactions are considered. Optimal catalyst preparation conditions were found in order to achieve maximum activity, and conceivable reasons for the effects of the above factors on the activity were revealed. The intermediate products and mechanisms of the photocatalytic and dark reactions of solutes that simulated chemical warfare agents in water are considered. All of the test simulants can undergo complete oxidation to form inorganic products in an aqueous TiO_2 suspension under irradiation with UV light. It was found that, in addition to oxidation, the dark steps of hydrolysis also play an important role in the degradation of these substances. The low-frequency ultrasonic treatment (20 kHz) of a photocatalyst suspension in the course of the photocatalytic oxidation of dimethyl methylphosphonate can accelerate the reaction because of the facilitated transport of reactants to the surface of photocatalyst particles.

Interest in heterogeneous photocatalytic processes has grown in the past decade. Thus, the number of scientific publications on this subject matter issued since 1991 is more than five thousands. Interest in these processes is due to several factors: First, photocatalytic or photostimulated reactions can occur at high rates at room temperature or even lower temperatures. Second, it was found that photocatalytic oxidation can degrade (mineralize) almost all organic compounds to inorganic products both in solutions and in a gas phase; this can be used for effective purification of the environment. Third, photocatalysts can efficiently operate on irradiation with visible light, including sunlight; this provides an opportunity to use solar energy for performing useful processes such as hydrogen generation from water. Finally, a number of organic synthesis reactions that can be performed in a single step only by photocatalysis became known [1].

The majority of test heterogeneous photocatalysts are semiconductors with various band gaps. Of these semiconductors, titanium dioxide is the most commonly used. This is due to its high catalytic activity, high chemical stability, inexpensiveness, and nontoxicity.

The principle of operation of semiconductor photocatalysts is currently represented by a schematic diagram shown in Fig. 1 using titanium dioxide as an example. The absorption of a light quantum in the bulk of a semiconductor results in electron transfer from the valence band to the conduction band. Then, the resulting electron–hole pair can form an exciton, recombine, or undergo separation followed by trapping of charge carriers at appropriate centers in the bulk of the semiconductor or on its surface. Conduction electron and hole exhibit pronounced redox properties and enter into reactions with the molecules or fragments of various compounds that occur on or at the surface of the semiconductor. These primary reactions initiate the subse-

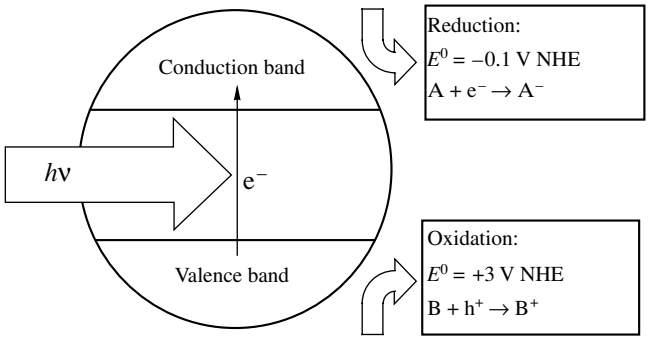

Fig. 1. Principle of operation of a TiO_2 catalyst: e^- and h^+ are photogenerated electrons and holes, respectively; E^0 are the corresponding standard electrode potentials of these species.

0023-1584/05/4602-0189 © 2005 MAIK "Nauka/Interperiodica"

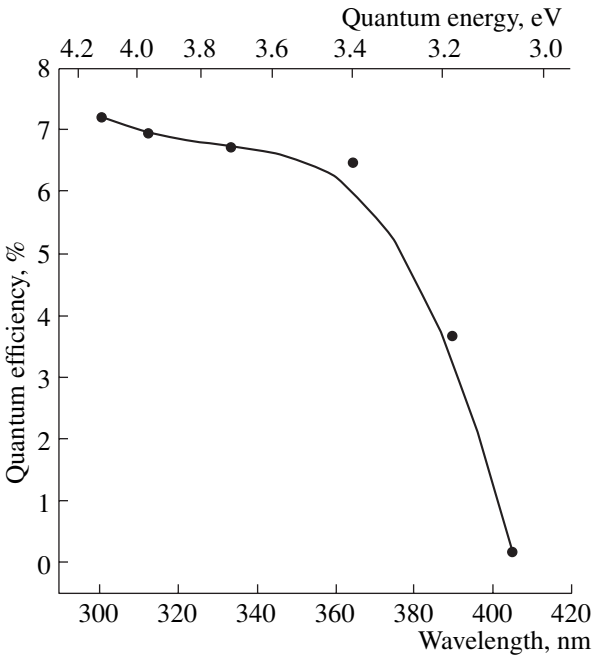

Fig. 2. Photocatalytic action spectrum of titanium dioxide (Hombikat UV 100) in the complete oxidation reaction of acetone vapor in a batch reactor. Reactor volume, 400 ml; initial concentration of acetone vapor, 550–700 ppm; monochromated light intensity on the sample, 0.3–0.4 W/m^2; sample surface area, 3 cm^2; the light wavelength was varied with an MDR-2 monochromator.

quent chains of chemical transformations, which can involve both dark reactions and reactions with photogenerated conduction electrons and holes.

It is believed that the photocatalytic oxidation of various substrates with molecular oxygen takes place after the primary reaction of photogenerated electrons with oxygen molecules, which results in a partial reduction to O_2^-, O_2^{2-}, and O^- [2]. Photogenerated holes react with water molecules to form extremely reactive $OH^\bullet$ radicals and directly react with the oxidized substrate and the above charged oxygen species. The active oxygen-containing species thus formed react with the oxidized substrate and initiate its further conversion up to the complete mineralization of the substrate.

To support the semiconductor nature of the photocatalytic activity of TiO_2, Fig. 2 demonstrates the experimental dependence of the quantum efficiency of acetone oxidation on the wavelength of irradiation light. It is well known that the band gap of TiO_2 is ~3.1 eV. It can be seen in Fig. 2 that the photocatalytic oxidation of acetone occurred with an almost constant quantum efficiency on short-wavelength irradiation and terminated on irradiation with light with photon energy lower than 3.1 eV. Thus, the above action spectrum is consistent with the statement that TiO_2 photocatalysis is of a semiconductor nature.

In this work, we summarized the results of our recent experimental studies on the preparation of active photocatalysts based on TiO_2 by thermal treatment and surface modification and the results of the photocatalytic oxidation of substances that simulate chemical warfare agents in water.

EXPERIMENTAL

In this study, we used Degussa P25 titanium dioxide with surface areas of 50 and 75 m^2/g (70% anatase and 30% rutile), Hombikat UV 100 (100% anatase; Sachtleben Chemie GmbH) with a surface area of 340 m^2/g, and independently prepared titanium dioxide samples (100% anatase). The oxidized organic substrates were of at least 95% purity. As a rule, photocatalytic oxidation was performed with oxygen of prepurified air.

Test reactions for the determination of photocatalytic activity in a gas phase were performed in flow-circulation and batch reactors equipped with optical quartz windows for the irradiation of photocatalysts. The degradation reactions of chemical warfare agent simulants were performed and the activity of photocatalysts in the liquid-phase oxidation of phenol was determined in batch reactors. Irradiation was performed with filtered or unfiltered light from a 1000-W xenon lamp or with unfiltered light from a 1000-W DRSh mercury lamp.

The reactants and products were analyzed by gas chromatography, gas chromatography–mass spectrometry (GC–MS), and ion chromatography. Total organic carbon (TOC) in aqueous solutions was determined with the use of an automated TOC analyzer (Shimadzu). To determine nonvolatile substances by GC–MS, they were converted into volatile species by reactions with bis(trimethylsilyl)trifluoroacetamide (Supelco).

The UV and visible spectra were recorded with the use of a UV-300 spectrophotometer (Shimadzu). In the measurements of diffuse-reflectance spectra, MgO was used as a standard substance. Upon irradiation with monochromated light with $\lambda = 313$ nm, incident light was almost completely absorbed by the samples of pure and modified TiO_2. Therefore, the quantum yields of a number of photocatalytic oxidation processes were calculated based on the intensity of incident light. The integrals of the diffuse-reflectance spectra of titanium dioxide samples were calculated from the equation $I = \int_{\lambda_1}^{\lambda_2} E(\lambda)d\lambda$, where $E(\lambda)$ is the reflectance (%) of light with wavelength λ (nm); and $\lambda_1 = 300$ nm and $\lambda_2 = 900$ nm are the limits of the range of measurement of diffuse-reflectance spectra.

The light flux intensity upon irradiation of a photocatalyst in reactors was determined by standard ferrioxalate actinometry or by using radiant power meters. The experimental procedure was considered in more detail in the publications cited.

RESULTS AND DISCUSSION

In this section, we consider the results of our studies oriented towards the development of active photocatalysts for liquid-phase and gas-phase oxidation as well as photocatalytic water-treatment technology. These studies involved preparation and characterization of photocatalysts and the kinetics and mechanisms of the oxidation of model substances.

1. Effect of the Preparation Procedure on the Activity of Photocatalysts Based on Titanium Dioxide

The preparation conditions of photocatalysts based on titanium dioxide have an extremely significant effect on catalyst activity. The effects of preparation factors such as the calcination temperature of amorphous TiO_2 samples, the procedure of supporting a platinum activator onto crystalline TiO_2, and the acid–base treatment of crystalline TiO_2 are considered below.

1.1. Effect of calcination temperature on the activity of titanium dioxide. The hydrolysis of titanium salts followed by thermal treatment of the resulting amorphous precipitate of metatitanic acid is one of the most commonly used procedures for the preparation of highly dispersed crystalline titanium dioxide. We found that the calcination temperature of samples prepared by the hydrolysis of $TiCl_4$ in an aqueous NH_3 solution had a great effect on the activity of the samples in the photocatalytic oxidation reaction of gaseous acetone [3]. As the calcination temperature was increased from 320 to 500°C, the specific surface area of TiO_2 decreased from 120 to 88 m^2/g. In this case, according to XRD and TEM data, the average size of TiO_2 crystallites increased from 11 to 17 nm. For all of the samples, only crystalline anatase was present and an amorphous phase was not detected. As the calcination temperature was increased to 450°C, the quantum yield of acetone oxidation initially increased from 15 to 41% and then decreased to 32% at a calcination temperature of 500°C.

To find a correlation between the physicochemical properties and the activity of TiO_2, we studied various spectroscopic characteristics of the test samples of TiO_2. Thus, the EPR spectra of these samples always exhibited a signal due to isolated paramagnetic NO molecules on the surface and in the bulk of TiO_2 [3]. The intensity of this signal monotonically increased with calcination temperature. Obviously, the molecules of NO are formed by the oxidation of residual NH_3 molecules upon calcination of the samples, and they are not directly related to changes in the photocatalytic activity with calcination temperature.

A more interesting behavior was found in the measurement of the diffuse-reflectance spectra of the samples in the visible and UV regions. All of the samples exhibited similar spectra, which are characteristic of semiconductors with a band gap of ~3 eV: complete light absorption was observed in the short-wavelength region, whereas the major portion of incident light was almost completely reflected at $\lambda > 400$ nm. It was found that reflection in the visible region of the spectrum correlated with the activity of the samples. Figure 3 shows that the integrals of diffuse-reflectance spectra (total whiteness) were linearly correlated with the quantum yield of the complete oxidation of acetone vapor. The occurrence of this correlation was also demonstrated in other series of samples prepared at various calcination temperatures [4]. Thus, this correlation can be used for a rapid search for the most active sample in a series with different calcination temperatures. It is likely that the nature of the correlation observed is related to competition between two opposite trends, which affect both the optical characteristics and the photocatalytic properties of TiO_2, as the calcination temperature is increased: an increase in surface crystallinity and the removal of surface hydroxyl groups. An increase in the degree of crystallinity of TiO_2 usually leads to an increase in photocatalytic activity, whereas the removal of surface hydroxyl groups causes a decrease in activity.

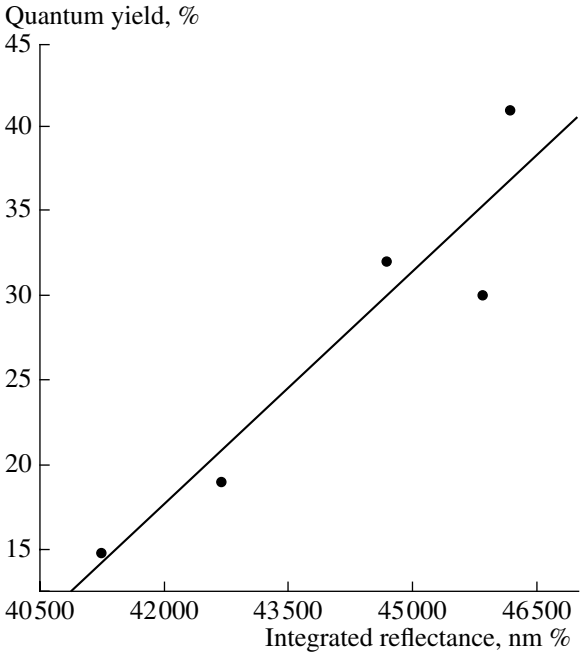

Fig. 3. Dependence of the quantum yield of the photocatalytic oxidation of acetone vapor in air on the integral of diffuse-reflectance spectra of titanium dioxide samples. The procedure used for calculating the integral of spectra is specified in the Experimental section.

1.2. Effect of supported platinum on the activity of titanium dioxide. Surface modification with noble metals, in particular, platinum, is a commonly used procedure for improving the photocatalytic properties of titanium dioxide. It is commonly believed that an increase in the photocatalytic activity after supporting platinum is primarily due to an improvement in photogenerated primary charge separation and a decrease in

Table 1. Activity of platinized photocatalysts based on TiO_2 (Fluka) prepared by the photoreduction of H_2PtCl_6

Phase composition	Platinum concentration, at. %	Platinum particle size, nm	Quantum yield of acetone oxidation*, %	Quantum yield of CO oxidation*, %
$PtO_2 + Pt(OH)_2/TiO_2$	1.2	0.8–1.6	2.8 (<0.5)	0.9 (<0.2)
$Pt(OH)_2/TiO_2$	1.5	0.5–7	5.5 (<0.5)	1.6 (0.9)
Pt^0/TiO_2	0.8	3	33 (1.4)	1.2 (<0.2)
PtO_2	29	6×50	1.4 (<0.5)	(32)
PtO_2/TiO_2, mechanical mixture	10	10–30	4.2 (<0.5)	(34)
TiO_2	0	TiO_2 58–300	30 (<0.5)	0.6 (<0.2)

Note: Temperature, 40°C; concentration of acetone vapor, 550 ppm; concentration of CO, 4200 ppm; intensity of monochromated light with $\lambda = 313$ nm, 7 mW/cm^2.

* The thermal activity of samples in the oxidation of acetone vapor, which was measured in the dark and, for convenience of comparison, expressed in the same units as the photocatalytic activity, is given in parentheses.

the rate of charge recombination. Another reason for the increase in activity can be the ordinary thermal catalytic activity of platinum, as both the starting substrates and their oxidation intermediates can undergo dark oxidation on platinum particles. Noble metals can be supported from their compounds onto TiO_2 using various techniques: by photocatalytic reduction in an aqueous, organic, or mixed suspension; by chemical reduction with gaseous hydrogen at elevated temperatures; and by chemical reduction with soluble mild reducing agents at room temperature. A change in the supporting procedure within a particular technique resulted in catalysts with strongly different activities.

Thus, in the photocatalytic deposition, metal particles were deposited at TiO_2 surface sites with an increased density of photogenerated electrons. It was found that the pH of the starting solution of H_2PtCl_6 had a strong effect on the oxidation state of deposited platinum: the lower the pH value, the lower the oxidation state of platinum. At pH < 4, platinum was deposited only as Pt^0 [5]. However, a decrease in pH strongly inhibited the photocatalytic deposition of platinum.

To study the effect of the state of supported platinum on the photocatalytic activity of TiO_2, we prepared the samples of TiO_2 (Fluka) modified with $Pt(OH)_2 + PtO_2$, PtO_2, and Pt^0 using a photocatalytic technique and a mechanical mixture of PtO_2 and TiO_2. Table 1 summarizes the results of the ESCA and TEM studies of the above samples and the photocatalytic activity of these samples in the gas-phase oxidation of acetone and CO [6]. It can be seen that the photocatalytic deposition technique resulted in the formation of platinum particles smaller than 7 nm. In this case, only the 0.8% Pt^0/TiO_2 sample exhibited higher activity in the photocatalytic oxidation of acetone. The quantum yield of the process measured on this sample was 33%, whereas the quantum yield on the parent TiO_2 was equal to 30%. In the oxidation of CO, all of the platinized samples were found to be more active than pure TiO_2. The 0.8% Pt^0/TiO_2 sample exhibited the greatest (twofold) increase in the purely photocatalytic activity in CO oxidation, as compared with pure TiO_2. The samples with high platinum contents were thermally active in CO oxidation, so that it was impossible to determine their activity in a photocatalytic reaction path.

The photocatalytic deposition of platinum onto Hombikat UV 100 titanium dioxide with a high specific surface area at pH 1.5 resulted in a photocatalyst with other properties. As a result of platinizing, the quantum yield of oxidation of acetone vapor on the above photocatalyst decreased from 62 to 39%, whereas the quantum yield of CO oxidation increased from 2 to 37% [7]. It is likely that great differences in the properties of platinized Fluka and Hombikat TiO_2 samples were due to a considerable difference between the specific surface areas of these titanium dioxides: 15 and 340 m^2/g, respectively.

The deposition of platinum onto titanium dioxide from an aqueous solution of H_2PtCl_6 with the use of chemical reduction with sodium borohydride should result in a photocatalyst exhibiting weaker contact between platinum particles and TiO_2 than that in the case of photocatalytic deposition. Indeed, the washing of a Pt/TiO_2 sample that was prepared by chemical reduction with distilled water resulted in the removal of a considerable portion of supported platinum [8]. A comparison between Pt/TiO_2 samples with similar platinum contents prepared by either chemical reduction or photoreduction demonstrated that the photocatalytic activity of the chemically reduced sample in the oxidation of gaseous acetone at 40°C was higher than that of the photoreduced catalyst by a factor of 1.5. An increase in the reaction temperature resulted in a continuous increase in the activity of platinized samples; in this case, the photocatalytic activities of the samples at 100°C also differed by a factor of 1.5. At 40°C, the photoplatinized catalyst exhibited a lower photocatalytic activity in the oxidation of acetone vapor, as compared with pure TiO_2.

The observed difference in the photocatalytic activity of photoplatinized and chemically platinized samples can be due to a difference in the interactions of titanium dioxide with supported platinum particles. In the photoplatinized sample, the contact of supported particles with the surface was more intimate; this fact may adversely affect the photocatalytic activity because of the enhanced recombination of photogenerated charge carriers.

Usually, improvement in the separation of photogenerated primary charges is considered among factors responsible for an increase in photocatalytic activity upon platinizing titanium dioxide. The greatest effect of platinum on this charge separation should be observed in photoplatinized TiO_2 because platinum particles in these samples are in intimate contact with the surface of the semiconductor. However, as demonstrated above, the occurrence of this contact actually resulted in a decrease in photocatalytic activity. By this it is meant that photocatalytically deposited platinum particles, which are in intimate contact with the catalyst, may in fact impair charge separation and accelerate charge recombination. The following factors can also be responsible for an increase in photocatalytic activity: (1) an improvement in the adsorption of a substrate on the surface of a photocatalyst, (2) thermal catalytic reactions on the surface of platinum particles, and (3) photocatalytic reactions directly on the surface of platinum particles. The effects of all of the above three factors were supported experimentally.

Thus, the constants of acetone adsorption from a gas phase on platinized TiO_2 were found to be higher than those on pure TiO_2 [8]. Thermal catalytic reactions were detected in the oxidation of acetone vapor away from light [8], as well as in acetone oxidation on a platinized catalyst coated with a thick layer of pure TiO_2 [9].

The photocatalytic oxidation of acetone directly on the surface of platinum particles was also detected. Thus, Fig. 4 shows the temperature dependence of the rate of complete acetone oxidation on platinized alumina under exposure to light and in the dark. It can be seen that the rates of oxidation under light and in the dark at 100 and 120°C were essentially different. Because alumina is photocatalytically inactive under irradiation with soft UV light, the observed difference in the rates should be ascribed to a photostimulated oxidation reaction on the immediate surface of platinum particles.

Impregnation with an aqueous solution of H_2PtCl_6 followed by reduction with hydrogen at elevated temperatures (300–400°C) is the most frequently used method for the deposition of platinum onto various supports. We studied the effect of the platinum thus deposited on the photocatalytic activity of Degussa P25 and Hombikat UV 100 TiO_2 in the oxidation reaction of phenol dissolved in water [10]. In this case, thermal reactions on platinum did not play a considerable role

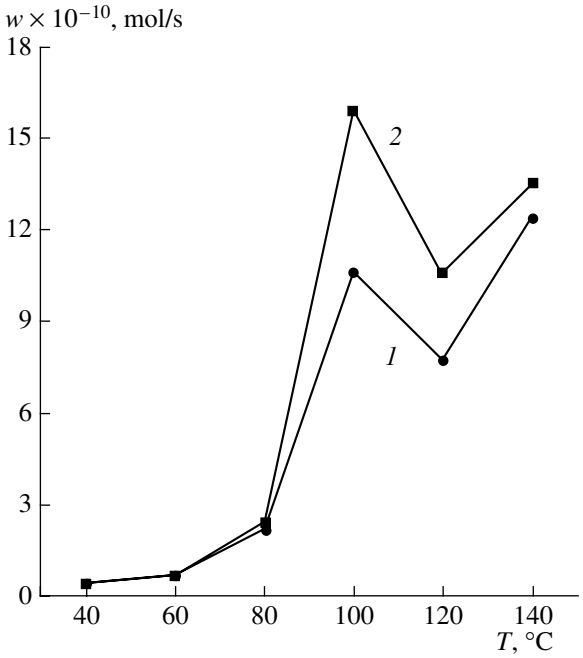

Fig. 4. Rates of oxidation (w) of acetone vapor in air on Pt/Al_2O_3 at various temperatures: (*1*) in the dark and (*2*) upon irradiation with UV light. The concentration of acetone vapor was 600 ppm, and the concentration of water vapor was 4500 ppm.

because the reaction was performed under thermostated conditions at a reduced temperature (12°C). It was found that an increase in photocatalytic activity was observed in the Hombikat TiO_2, whereas platinization of the Degussa TiO_2 only decreased the activity (Table 2). In the platinization of the Hombikat TiO_2, a sample with 1 wt % platinum exhibited the greatest photocatalytic activity. Nevertheless, the photocatalytic activity of this sample was lower than the activity of the pure Degussa TiO_2 by a factor of ~1.5. Transmission electron microscopy allowed us to find that the platinum particles prepared as described above were well dispersed over the surface of TiO_2 and measured 0.7–1 nm. The total surface area of the platinum particles deposited by the above method linearly increased with the amount of the supported metal [10]; this resulted in close contact between platinum particles and the catalyst and in an increase in the activity of the Hombikat TiO_2.

Unlike photoplatinization, the deposition of platinum from solution followed by reduction with hydrogen did not result in the precipitation of platinum particles at sites with an increased density of photogenerated electrons. Therefore, in this case, deposited platinum particles could additionally improve charge separation. However, because the initial sample of Degussa P25 TiO_2 exhibited a very high efficiency of photogenerated charge separation, supported platinum did not improve its photocatalytic activity. Platinization may also have an adverse effect because of the specific-

Table 2. Effect of the amount of supported platinum on the initial quantum efficiency of phenol oxidation in an aqueous suspension of the Pt/TiO_2 photocatalyst

TiO_2 Hombikat UV 100		TiO_2 Degussa P25	
platinum concentration, wt %	initial quantum efficiency, %	platinum concentration, wt %	initial quantum efficiency, %
0	0.12	0	0.88
0.5	0.26	0.1	0.79
1	0.43	0.25	0.63
1.5	0.36	0.5	0.59
2	0.31	1.5	0.48
3	0.34		

Note: Quantum efficiency upon irradiation with a 200-W mercury lamp at 12.5 ± 0.5°C was calculated by dividing the initial rate of reaction by the incident flux of light quanta.

ity of deposition by high-temperature reduction with hydrogen. Indeed, upon the deposition of platinum by chemical reduction, we found a considerable increase in the activity of the Degussa TiO_2 in the oxidation of dimethyl methylphosphonate dissolved in water.

1.3. Effect of the surface acidity of TiO_2 on photocatalytic oxidation. The change of the photocatalytic properties of TiO_2 by modifying surface acid–base sites is a relatively new area of heterogeneous photocatalysis [11]. It is of importance that the reactions of photogenerated conduction electrons and holes are strongly exothermal reactions and occur at a very high rate. It is likely that this rate does not limit the subsequent chemical transformations, which do not require light quanta. On the other hand, the dark steps of a reaction sequence of the oxidized substrate can depend on surface acidity, and their rates can considerably vary depending on reaction conditions.

Table 3 summarizes data on changes in the properties of Hombikat UV 100 titanium dioxide after treatment with aqueous solutions of sulfuric acid or sodium hydroxide at 60°C for 2 h. An increase in the concentration of sulfuric acid increased the amount of acid sites on the surface of TiO_2 and decreased the amount of basic sites. On treatment with sodium hydroxide, the same trend was observed with respect to basic sites. Acid–base treatment did not affect significantly the surface area and pore diameter of the test samples of TiO_2. At the same time, acid treatment resulted in a significant increase in the photocatalytic activity of TiO_2, whereas basic treatment resulted in a considerable decrease in this activity. A clear correlation between the quantum efficiency of the deep oxidation of gaseous acetone and the number of acid sites on the surface of TiO_2 was observed.

A probable reason for the observed increase in photocatalytic activity with increasing surface acidity of TiO_2 is the facilitated desorption of the resulting CO_2 as the final reaction step of complete oxidation. Indeed, Fig. 5 shows that the adsorption isotherms of carbon dioxide underwent a considerable change because of the treatment of titanium dioxide with a 1 M H_2SO_4 solution. In this case, the adsorption of CO_2 from dry air decreased by a factor of ~5. At high gas-phase humidity, the decrease in adsorption was much less significant. This was likely due to the complete coverage of the hydrophilic surface of TiO_2 with a water film at high air humidity and the inability of carbon dioxide molecules to displace adsorbed water from the surface. The high surface acidity facilitated the rapid degradation of surface carbonates; thus, it can accelerate this final step of complete oxidation.

The acid catalysis of one of the dark steps of complete oxidation can be another factor responsible for an increase in the activity. This is exemplified by the hydrolysis of dimethyl methylphosphonate. A rate-limiting step catalyzed by an acid site can provide a

Table 3. Effect of acid–base pretreatment on the properties and photocatalytic activity of Hombikat UV 100 titanium dioxide in the oxidation of acetone vapor

Solution composition for the treatment of TiO_2	Specific surface area S_{BET}, m^2/g	Pore diameter, nm	Amount of acid sites, 10^{-4} mol/g	Amount of basic sites, 10^{-3} mol/g	Quantum efficiency of oxidation of acetone vapor, %
10 M H_2SO_4	–	–	6.13	0.533	76
4 M H_2SO_4	341	5.0	5.10	0.639	71
1 M H_2SO_4	306	5.2	4.98	0.632	68
Untreated	347	4.9	3.69	0.982	62
1 M NaOH	–	–	3.00	1.12	44
4 M NaOH	355	5.0	2.60	1.29	30
10 M NaOH	–	–	1.74	1.32	17

Note: The photocatalytic tests were performed under the following conditions: temperature, 40°C; concentration of acetone vapor, 500 ppm; concentration of water vapor, ~5000 ppm; irradiation with light from a 1000-W xenon lamp filtered using an interference light filter (λ = 334 nm).

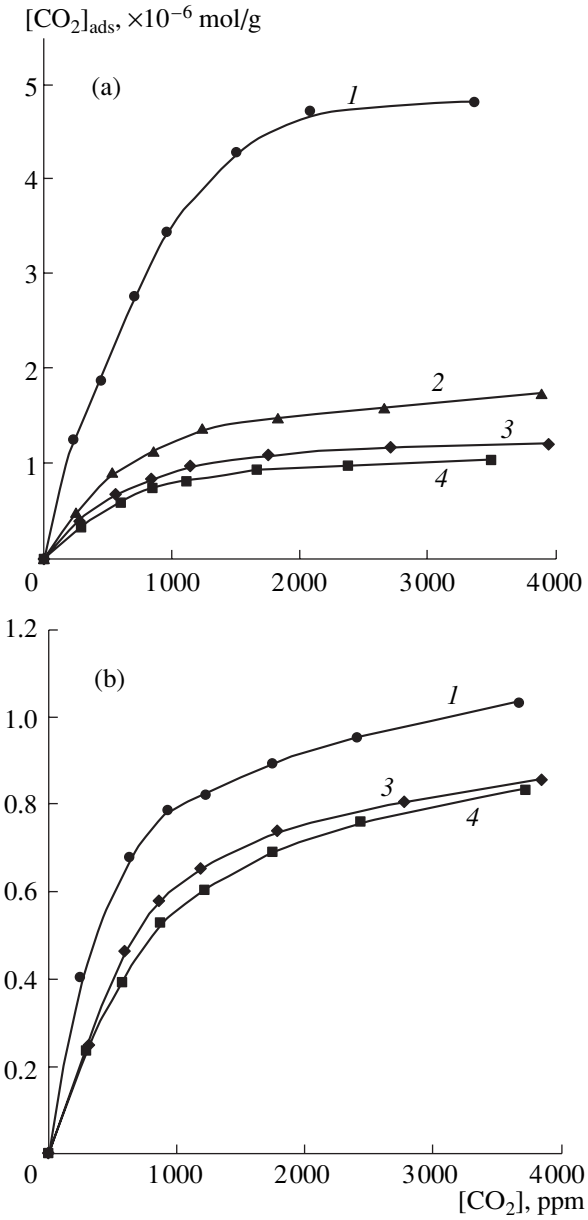

Fig. 5. Adsorption isotherms of gas-phase CO_2 on (a) pure Hombikat UV 100 TiO_2 and (b) the above TiO_2 treated with an aqueous 1 M H_2SO_4 solution. The isotherms were measured at room temperature and at the following pressures of water vapor, ppm: (*1*) 0 (relative humidity of the gas phase, 0%), (*2*) 7400 (25%), (*3*) 16000 (53%), and (*4*) 22200 (74%).

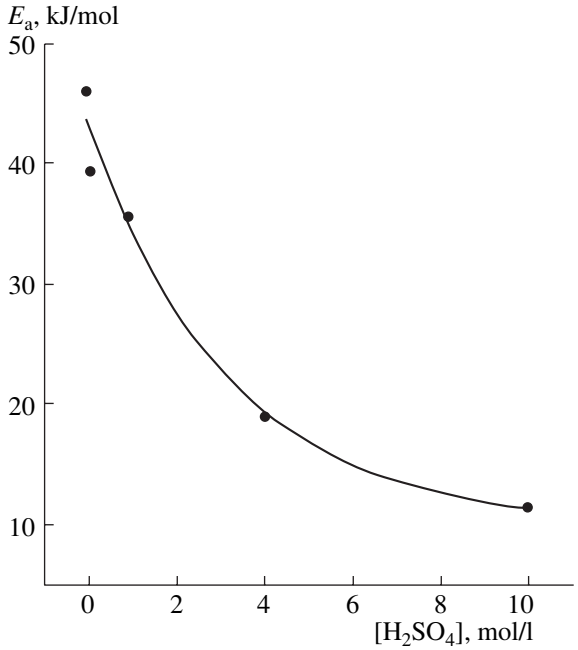

Fig. 6. Dependence of the apparent activation energy (E_a) of the photooxidation of benzene vapor in the air on the concentration of sulfuric acid used for the modification of Hombikat UV 100 TiO_2. Relative air humidity, 70–80%; room temperature; full UV-light intensity of a DRSh-1000 lamp, 10 mW/cm^2.

decrease in the apparent activation energy of oxidation and, consequently, accelerate the process of complete oxidation. Figure 6 demonstrates the effect of sulfuric acid on the apparent activation energy of the photocatalytic oxidation of benzene vapor in a gas phase [12]. An increase in the concentration of sulfuric acid used for the treatment of TiO_2 resulted in a monotonic decrease in the activation energy of the overall reaction. At a high acid concentration, the activation energy approached a value close to 10 kJ/mol. Thus, the acid treatment of a surface can decrease the activation energy by a factor of higher than 4.

2. Kinetics and Reaction Paths of Photocatalytic Oxidation

2.1. Complications of the apparent kinetics of catalytic and photocatalytic reactions in batch reactors. Both flow and batch reactors are used in studies and practical applications of photocatalytic oxidation. Under steady-state conditions in flow reactors, the amounts of reactants adsorbed on a photocatalyst remained constant; therefore, they can be ignored in a mass balance of the observed photocatalytic reactions. In batch reactors, the concentrations of reactants and products changed in the course of the reaction, and adsorbed substances should be taken into account in a mass balance. Thus, if a considerable fraction of reactants in a batch reactor occurs in an adsorbed state, the kinetics of changes in the measured concentrations of these substances in a gas or liquid phase can be significantly different from the case in which the main amounts of the reactants occur in a homogeneous gas or liquid phase in the reactor. This difference can be particularly important in the case of low-temperature heterogeneous catalytic processes, which are characteristic of heterogeneous photocatalysis.

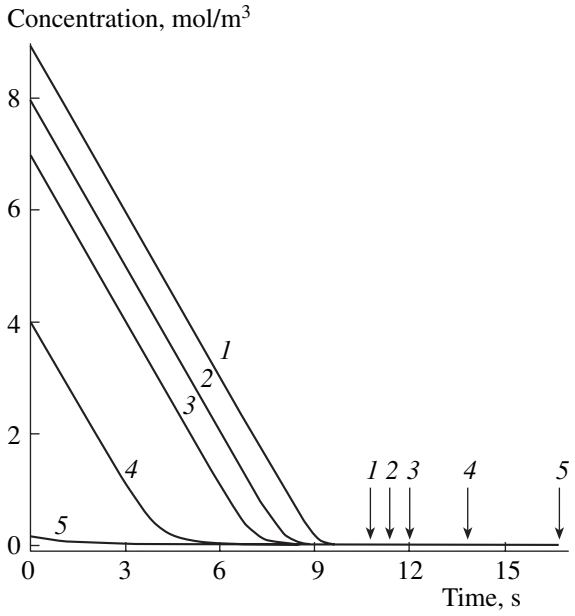

Fig. 7. Calculated kinetics of consumption of a substance in a batch reactor according to the Langmuir–Hinshelwood model at various amounts of adsorption sites on the surface of an inoperative catalyst, mol: (*1*) 0, (*2*) 1, (*3*) 2, (*4*) 5, and (*5*) 10. The amount of adsorption sites on a working catalyst was 1 mol, and the initial substance amount was 10 mol. The reactor volume was 1 m^3. Arrows indicate the attainment of a desired final substrate concentration of 5 $mmol/m^3$.

As the simplest example, we consider a photocatalytic first-order reaction, which obeys the Langmuir–Hinshelwood equation and takes place with the participation of large amounts of a catalyst [13]. Let us assume that S_i reaction sites are irradiated with light and the photocatalytic reaction occurs at these sites, whereas S_n reaction sites on the surface of the photocatalyst are not illuminated and they operate as an adsorbent. For simplicity, assume that the equilibrium constants of adsorption (K) are equal for illuminated and darkened active sites. The total number of moles (n) of an initial substance (a substrate of the photocatalytic reaction) in the test system obeys the balance equation

$$n = cV + \frac{(S_i + S_n)Kc}{1 + Kc}, \qquad (1)$$

where c is the substrate concentration in a homogeneous liquid or gas phase in the reactor, and V is the volume of this phase.

On the other hand, the total substrate amount in the system changes only because of a surface reaction. In the simplest case, the rate of this change is described by the Langmuir–Hinshelwood equation

$$\frac{dn}{dt} = -\frac{S_i kKc}{1 + Kc}, \qquad (2)$$

where k is the apparent rate constant of the surface reaction.

Differentiating Eq. (1) with respect to time and then equating it to (2), we can find the rate of change in the substrate concentration in a homogeneous phase in the reactor:

$$\frac{dc}{dt} = \frac{-\dfrac{S_i kKc}{1 + Kc}}{V + \dfrac{(S_i + S_n)K}{(1 + Kc)^2}}. \qquad (3)$$

Thus, the occurrence of adsorption in the system always affects the apparent kinetics of changes in the substrate concentration in the volume of a batch reactor. When the main amount of the converted substrate is not adsorbed, the second term in the denominator of Eq. (3) can be ignored and the kinetics of changes in the substrate concentration in a homogeneous phase is reduced to the traditional Langmuir–Hinshelwood kinetics.

The above circumstance is of particular importance for heterogeneous photocatalysis because a considerable portion of the surface of a photocatalyst can be unilluminated under real conditions. Thus, this portion of the surface can participate only in adsorption processes. Evidently, the kinetics is affected by changes in the fraction of the unilluminated portion of the photocatalyst. Figure 7 shows concentration profiles calculated from Eq. (3) at a fixed initial substrate amount in the reactor depending on the amount of darkened adsorption sites in the photocatalyst. It can be seen that the initial substrate concentration in a homogeneous phase in the reactor decreased with increasing area of the unilluminated photocatalyst surface, whereas the time taken to reach a given low finite concentration of the substrate in the homogeneous phase increased. Although the kinetics of substrate concentration considerably changed, the experimental kinetic curves can be adequately approximated by the simplest Langmuir–Hinshelwood kinetics. Nevertheless, the parameters obtained by a corresponding optimization of the experimental kinetic curves can differ from true values by a small factor [13].

In the practical use of photocatalysis for the purification of a liquid or gas phase, the usual challenge is to decrease the concentration of the photooxidized substrate (a pollutant in air or water) to a level lower than a certain value (for example, the maximum permissible concentration (MPC) of the substrate) in the shortest possible time. If the MPC is sufficiently high, the addition of an amount of a heterogeneous photocatalyst may remove the pollutant from the bulk by adsorption even before oxidation. At the same time, at low MPC values, the time taken to reach a pollutant concentration lower than the MPC can significantly increase with the used amount of a photocatalyst (Fig. 7).

2.2. Photocatalytic oxidation in solutions. The photocatalytic oxidation of compounds in solutions is

widely used for the purification and disinfection of water containing trace organic and inorganic pollutants. Unlike traditional catalytic processes, this oxidation usually does not require additional water heating and/or the addition of reagents to the system. In this section, we consider the photocatalytic degradation of substances that simulate highly toxic compounds: chemical warfare agents.

2.2.1. Degradation of 2-phenethyl 2-chloroethyl sulfide on TiO_2. The test compound contains the SCH_2CH_2Cl group, which is present in the chemical warfare agent yperite (mustard gas). Because of the presence of a phenyl substituent, the toxicity of the simulant is low (LD_{50} of 850 mg/g in mice). Similarly to yperite, the simulant is sparingly soluble in water, and its dissolution is accompanied by hydrolysis. Figure 8 illustrates the kinetics of hydrolysis and photocatalytic oxidation of the simulant [14]. It can be seen that, upon the addition of the simulant to an aqueous suspension of TiO_2, the TOC concentration in solution slowly increased, and this increase was accompanied by a decrease in pH and an increase in the concentration of chloride ions. Thus, the dissolution of the simulant in water was accompanied by the hydrolysis of the C–Cl bond.

Upon the onset of irradiation of the suspension with full light from a medium-pressure mercury lamp, the TOC content rapidly decreased and the concentration of sulfate ions in the aqueous phase of the suspension increased. After irradiation for approximately 4 h, the aqueous phase of the solution contained almost no organic compounds, whereas the detected concentration of sulfate ions (120 mg/l) corresponded to the complete mineralization of the simulant. To find the contribution of possible direct uncatalyzed photolysis of the simulant, we studied its photocatalytic oxidation under exposure to light from a mercury lamp passed through a Pyrex filter with a transmission band at $\lambda > 300$ nm. Under these conditions, the direct light absorption by simulant molecules was excluded because the red threshold of its absorption is near 275 nm. In this case, photocatalytic oxidation occurred at a rate ~10 times lower than that on irradiation with unfiltered light. A very high rate of photolysis was observed upon the irradiation of the system with full light from a mercury lamp in the absence of TiO_2: the TOC concentration in the aqueous phase decreased to almost zero in 185 min. Upon irradiation with filtered light, direct uncatalyzed photolysis was not observed.

Practically the same products were detected in both direct photolysis and photocatalytic oxidation. Styrene, benzaldehyde, and benzeneacetaldehyde were predominant among the volatile products of degradation. The nonvolatile products that remained in the aqueous phase contained 2-phenethyl 2-hydroxyethyl sulfide, 2-phenethyl 2-hydroxyethyl sulfone, 2-phenethylsulfinic acid, benzeneacetic acid, benzoic acid, etc. Considerable amounts of 2-phenethyl disulfide,

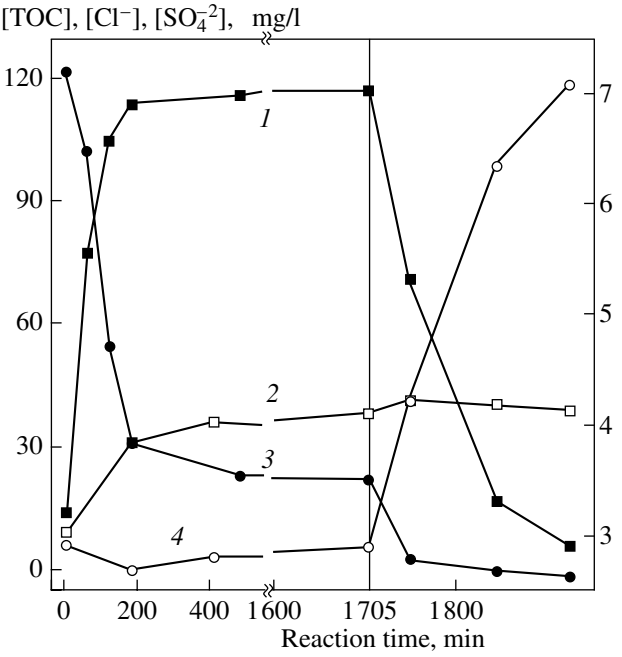

Fig. 8. Kinetics of changes in the concentrations and pH of an aqueous phase in the hydrolysis and subsequent photocatalytic degradation of a yperite simulant (2-phenethyl 2-chloroethyl sulfide) in an aqueous suspension of Hombikat UV 100 TiO_2: (*1*) TOC, (*2*) chloride ions, (*3*) pH, and (*4*) sulfate ions. Initial simulant concentration, 250 mg/l; TiO_2 concentration, 250 mg/l; UV irradiation with a 450-W mercury lamp started after 1705 min.

2-phenethylsulfinic acid, and 2-phenethyl trisulfide were extracted from the surface of the photocatalyst after the reaction. Figure 9 demonstrates possible reaction paths of the photostimulated degradation of the simulant, which follow from the nature of degradation products. After a dark step (which does not require the participation of light) of hydrolysis of the carbon–chlorine bond, the photocatalytic or photolytic cleavage of carbon–sulfur bonds took place, followed by the oxidation and hydrolysis of the products up to the formation of the final inorganic substances: sulfuric acid, carbon dioxide, and hydrogen chloride.

2.2.2. Effect of ultrasound on the photocatalytic oxidation of dimethyl methylphosphonate. The photocatalytic oxidation of substrates in aqueous suspensions usually occurs at much lower rates than the corresponding gas-phase processes. Nevertheless, in the oxidation of heteroatomic organic substances, a liquid-phase process is usually characterized by lower deactivation of the photocatalyst. This is due to the fact that the final inorganic products of oxidation desorb into solution and do not block surface reaction centers. It is well known that ultrasound can initiate a number of oxidation reactions and accelerate photocatalytic reactions in a liquid phase.

We studied the effect of 20-kHz ultrasound on the photocatalytic degradation of dimethyl methylphos-

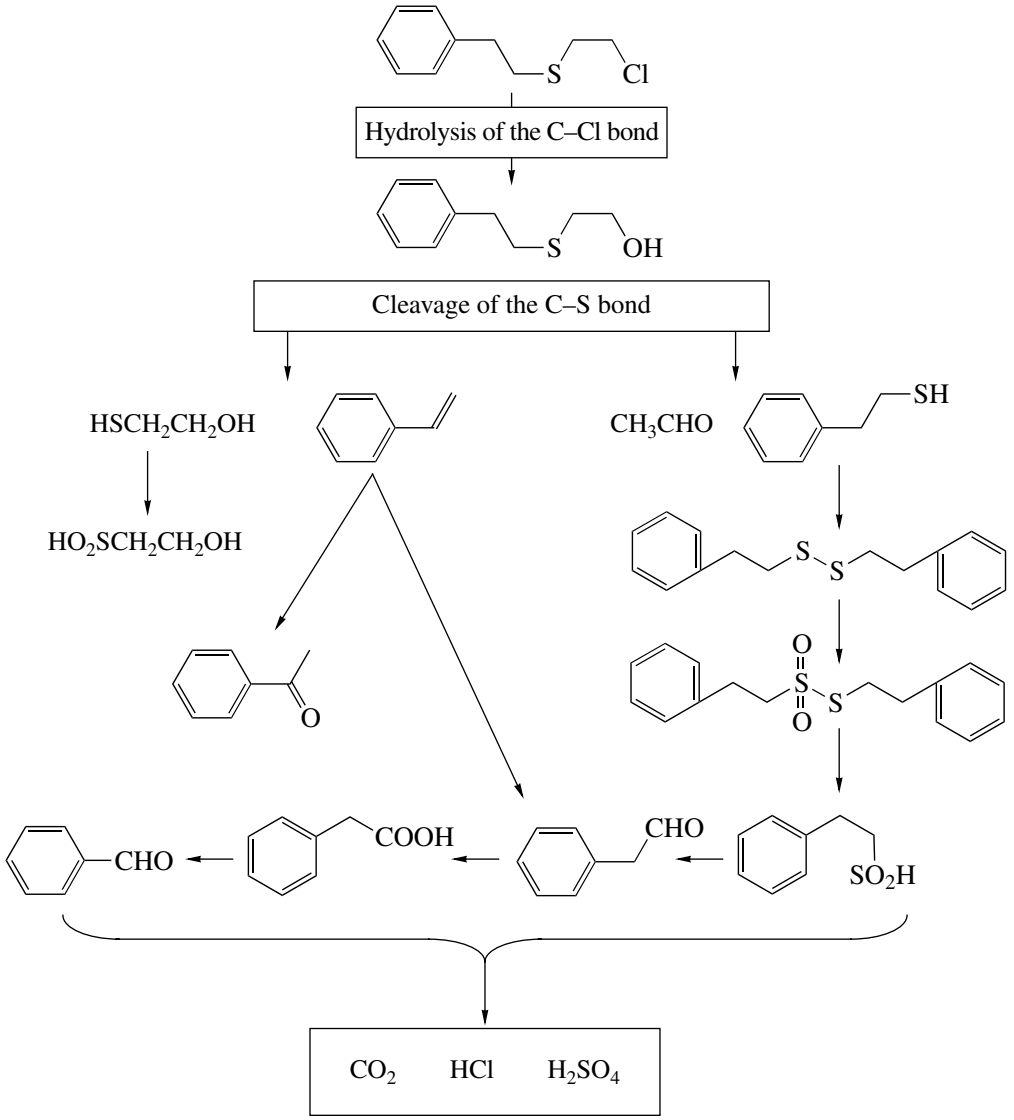

Fig. 9. Conceivable reaction scheme of the degradation of 2-phenethyl 2-chloroethyl sulfide in an aqueous suspension of Hombikat UV 100 TiO_2 under UV irradiation.

phonate in a batch reactor [15]. Figure 10 shows the curves that characterize TOC concentration changes in solution under various oxidation conditions. It can be seen that the oxidation of dimethyl methylphosphonate in a suspension of the Hombikat UV 100 TiO_2 photocatalyst did not occur under the action of only ultrasound (curve *1*). In the photocatalytic oxidation of dimethyl methylphosphonate in the absence of ultrasound (curve *3*), the TOC concentration decreased at an average rate of 0.15 mg l^{-1} min^{-1}. Upon the simultaneous ultrasonication and UV irradiation of the suspension, the oxidation of dimethyl methylphosphonate was considerably accelerated, and the rate of TOC consumption was as high as 0.34 mg l^{-1} min^{-1}. The following factors may be responsible for the positive effect of ultrasound: (1) an increase in the dispersity of TiO_2 particles in the suspension, (2) a facilitated transport of reactants due to improved stirring of the suspension, and (3) a change in the reaction mechanism. Curve *2* in Fig. 10 was measured under conditions of short-time exposures to ultrasound at regular intervals for dispersing the photocatalyst. In this case, the reaction rate of dimethyl methylphosphonate oxidation was somewhat lower than that in the photocatalytic oxidation without ultrasonication. Consequently, an increase in the dispersity of TiO_2 is not the main reason for the positive effect of ultrasound. Indeed, the intensification of stirring of the suspension on photocatalytic oxidation resulted in a small increase in the rate of dimethyl methylphosphonate oxidation (curve *4*). Thus, a conceivable reason for the positive effect of ultrasound consists in an acceleration of reactant transport to the surface of TiO_2.

To study the possible effect of ultrasound on the mechanism of photocatalytic oxidation, we identified

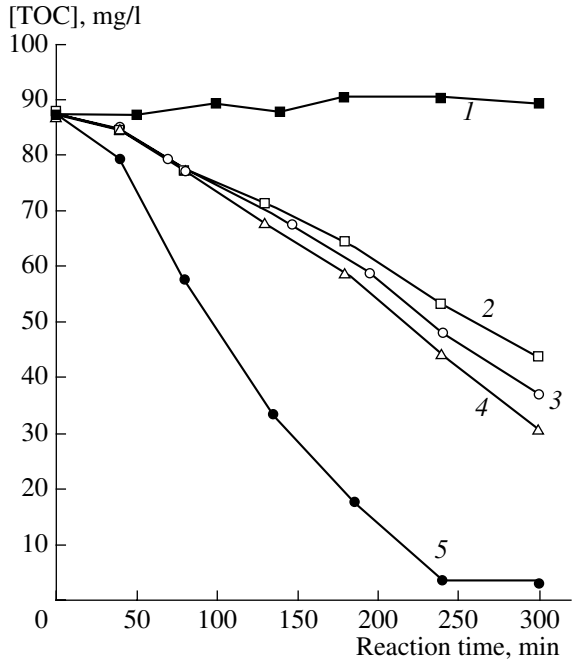

Fig. 10. Kinetics of changes in the concentration of TOC in the oxidation of dimethyl methylphosphonate in an aqueous suspension of Hombikat UV 100 TiO_2: (*1*) under the action of 20-kHz ultrasound, (*2*) under UV irradiation with ultrasonication at regular intervals in the dark, (*3*) under UV irradiation, (*4*) under UV irradiation with stirring with a magnetic stirrer, and (*5*) under UV irradiation with ultrasonication. In all cases, a flow of air (500 cm^3/min) caused stirring to prevent the sedimentation of TiO_2 from the suspension. Irradiation was performed with unfiltered light from a 450-W mercury lamp.

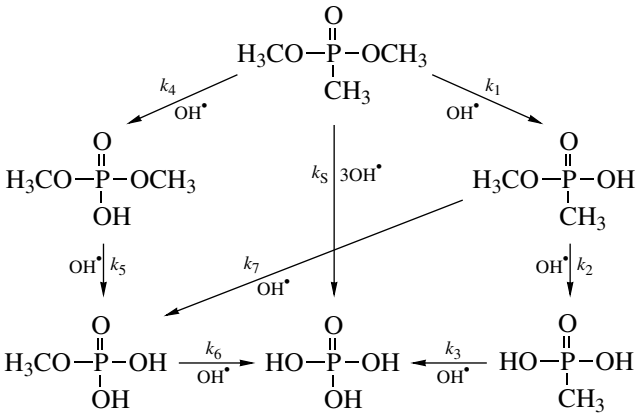

Fig. 11. Detected products and conceivable reaction paths in the photocatalytic degradation of dimethyl methylphosphonate in an aqueous suspension of Hombikat UV 100 TiO_2. The reaction conditions are specified in Fig. 10.

the degradation products of dimethyl methylphosphonate and measured their relative concentrations. We detected five reaction products: the three main products were phosphate ions, methyl methylphosphonate, and methylphosphonate, and the two other products, dimethyl phosphate and methyl phosphate, were present in lower concentrations.

Figure 11 shows the reaction scheme of the photocatalytic oxidation of dimethyl methylphosphonate, which was constructed based on the experimental data on reaction products. It is believed that hydroxyl radicals generated on TiO_2 initiate the oxidation of the initial substrate and detected intermediates. After this initiation, several subsequent steps of oxidation rapidly occur with the participation of atmospheric oxygen and without the participation of light. We constructed a kinetic model for the oxidation scheme proposed. The adequacy of this model was checked against experimental kinetics of the photocatalytic oxidation of dimethyl methylphosphonate and the intermediates and products of this oxidation [15]. It was found that the optimized values of all of the rate constants used in this model for photocatalytic oxidation in the presence of ultrasound were higher than those in the absence of ultrasound. As expected, this can be easily explained by an accelerated reactant transport under the action of ultrasound.

The kinetics of the photocatalytic oxidation of dimethyl methylphosphonate in the absence of ultrasound is adequately described by a reaction scheme without a step of the direct oxidation of dimethyl methylphosphonate to phosphate ions with constant k_S. However, this step should be added in order to describe satisfactorily the reaction kinetics in the presence of ultrasound. Thus, the action of ultrasound results in the appearance of an additional oxidation reaction path, which can be related, for example, to a considerable acceleration of the transport of reactants into the pores of the photocatalyst. If the starting compound (dimethyl methylphosphonate) enters into the micropores of the photocatalyst, it can occur there up to complete photocatalytic oxidation. Therefore, in terms of the detection of the concentration of the starting substrate in a homogeneous aqueous phase, the complete oxidation of dimethyl methylphosphonate to phosphate ions within pores without the release of intermediate products into the bulk of the solution appears as a step with rate constant k_S (Fig. 11).

2.2.3. Photocatalytic degradation of other chemical warfare agent simulants. We also studied the conversion of diethylphosphoramidate, pinacolyl methylphosphonate, and 2-(butylamino)ethanethiol [16], which simulate the chemical structures of the chemical warfare agents tabun, soman, and VX, respectively.

Figure 12 shows the kinetics of decrease in the concentration of TOC during the oxidation of the above substances in an aqueous suspension of Hombikat UV 100 TiO_2 in a batch reactor under exposure to light from a xenon lamp. At equal initial concentrations of the simulants (250 mg/l), the highest and lowest rates of complete oxidation were observed with pinacolyl methylphosphonate and 2-(butylamino)ethanethiol, respectively. It can be seen that all of the simulants

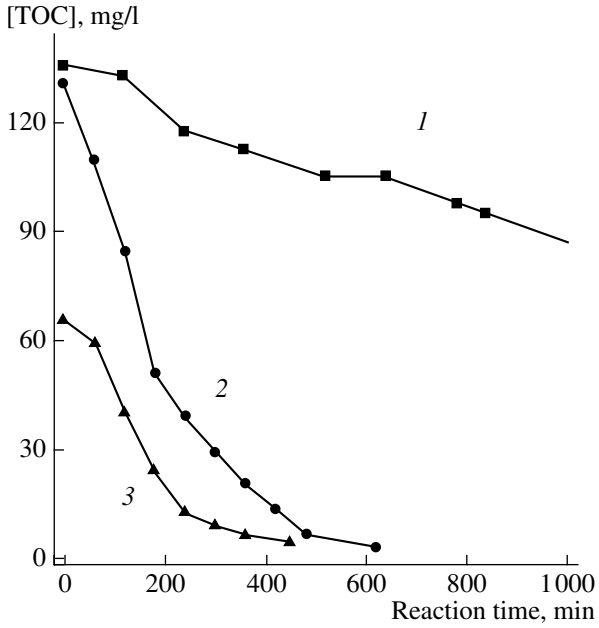

Fig. 12. Kinetics of changes in the concentration of TOC in the photocatalytic degradation of substances that simulate chemical warfare agents in an aqueous suspension of Hombikat UV 100 TiO_2: (*1*) 2-(butylamino)ethanethiol, (*2*) pinacolyl methylphosphonate, and (*3*) diethylphosphoramidate. The initial concentrations of all of the substances and TiO_2 were 250 mg/l.

under discussion underwent complete mineralization to inorganic substances.

In the course of the photocatalytic degradation of diethylphosphoramidate, an increase in the concentrations of ammonium, nitrate, and phosphate ions in the aqueous phase of the suspension was detected. Nitrite ions in a low concentration were also detected. After completion of the photocatalytic oxidation of the simulant, the concentration of nitrite ions decreased to a very low value. Three fourths of the nitrogen in the starting simulant was converted into ammonia as a result of oxidation. Among volatile reaction products, acetaldehyde and ammonia were detected, whereas nonvolatile products contained seven compounds.

The composition of the products and kinetic data on the photooxidation allowed us to propose a scheme of reaction paths, which is shown in Fig. 13. All of the products specified in this reaction scheme were detected experimentally. The main reaction paths are the photocatalytic oxidation of the α-carbon atom followed by the hydrolysis of the resulting anhydride/hemiacetal and the cleavage of the phosphorus–nitrogen bond, which mainly leads to ammonia. In the course of the subsequent reactions, the photocatalytic and dark oxidation of other moieties of the substrate molecule and the formation of inorganic products take place.

In the oxidation of pinacolyl methylphosphonate, methylphosphonic acid was the main nonvolatile reaction intermediate, whereas acetone was the main volatile product. An additional 11 volatile products, which were formed by the oxidation of the pinacolyl residue of the parent substance, were found in lower concentrations. Among nonvolatile products, an additional 8 substances were detected aside from methylphosphonic acid. Figure 14 demonstrates the scheme of the initial reaction paths of the photocatalytic oxidation of pinacolyl methylphosphonate. It is believed that the dark oxidation of the simulants under consideration is initiated by the reaction of a substrate with the photocatalytically generated hydroxyl radical. Next, the resulting alkyl radicals react with molecular oxygen to form alkylperoxide radicals; alcohols and aldehydes can be formed by subsequent conversion of the latter radicals.

The pinacolyl methylphosphonate molecule contains three types of carbon atoms, which can be readily attacked by hydroxyl radicals (Fig. 14). Thus, in the photocatalytic oxidation of the CH group, the constituent hydrogen is replaced by the hydroxyl group. In this case, the simulant molecule is converted into a hemiacetal, which, as is well known, is readily hydrolyzed in aqueous solutions. This hydrolysis results in methylphosphonic acid and pinacolyl alcohol.

The photocatalytic oxidation of the methyl groups of a *tert*-butyl moiety results in the formation of corresponding alcohol, aldehyde, and acid, whereas the oxidation of the methyl group bound to phosphorus primarily gives pinacolylphosphoric acid. Finally, all of the intermediate products are oxidized to carbon dioxide and phosphoric acid.

The most interesting products were found in the photocatalytic oxidation of 2-(butylamino)ethanethiol. This simulant contains the S–CH_2CH_2–N moiety, which is characteristic of the chemical warfare agent VX. In the photocatalytic oxidation of this substrate in an aqueous suspension of TiO_2, an increase in the concentrations of sulfate and ammonium ions was observed. The concentration of nitrite ions passed through a maximum at reaction times of ~100 min and then decreased, whereas the concentration of nitrate ions remained low during the entire course of the reaction (650 min). Although the TOC concentration decreased by only 29% in 650 min, the concentration of the resulting sulfate ions corresponded to a 66% conversion of the total sulfur of the parent substance. We detected 22 volatile and 14 nonvolatile intermediates. The most interesting products were volatile heterocyclic compounds containing sulfur and nitrogen in the rings, such as 2-propyldihydrothiazole *S*-oxide, 2-propylthiazoline, 2-propylthiazole, and 2-propylthiazolidine.

Figure 15 shows the scheme of the initial reaction paths of this simulant, which was constructed based on the composition of the main products detected. As in the case of other sulfur-containing compounds, one of

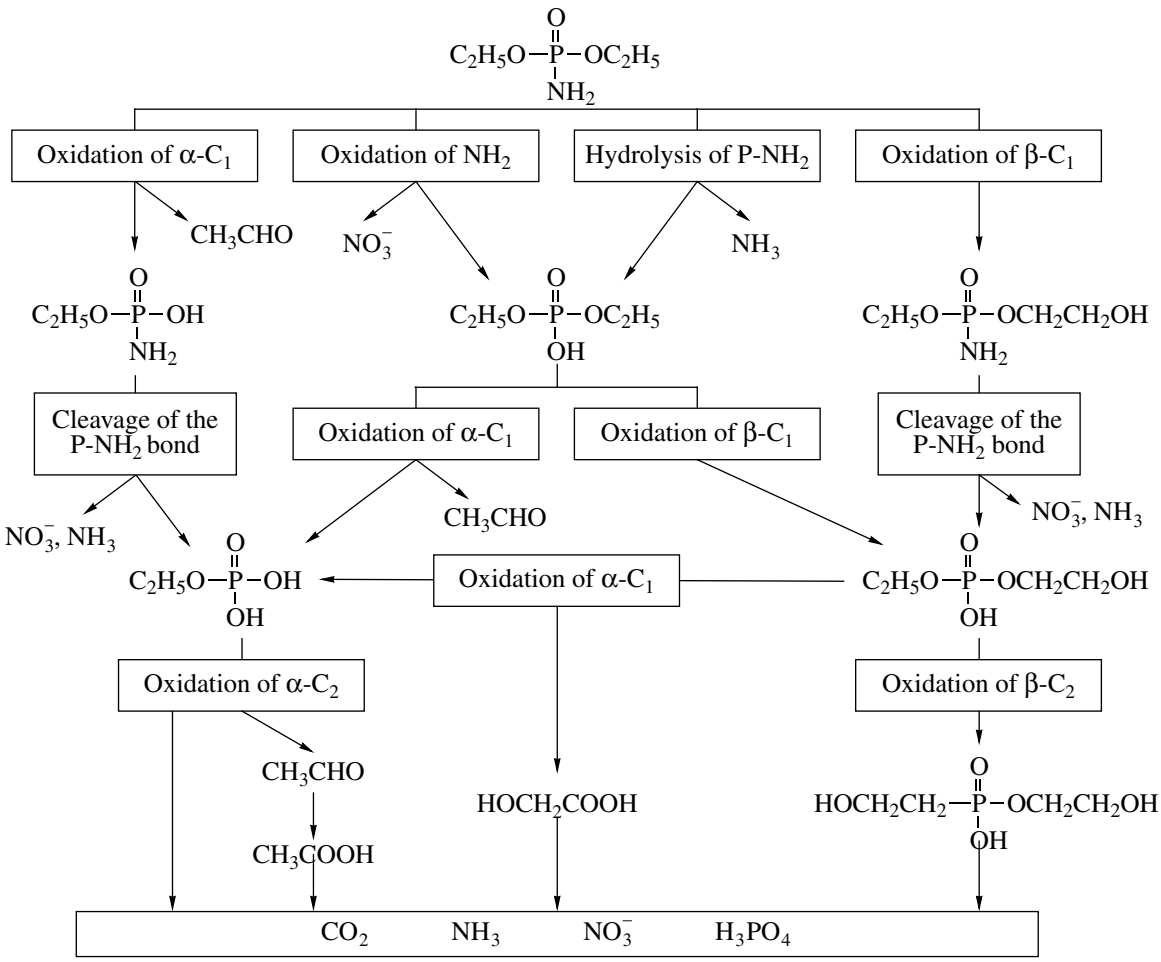

Fig. 13. Detected products and a conceivable scheme of the main reaction paths in the photocatalytic degradation of diethylphosphoramidate in an aqueous suspension of Hombikat UV 100 TiO_2.

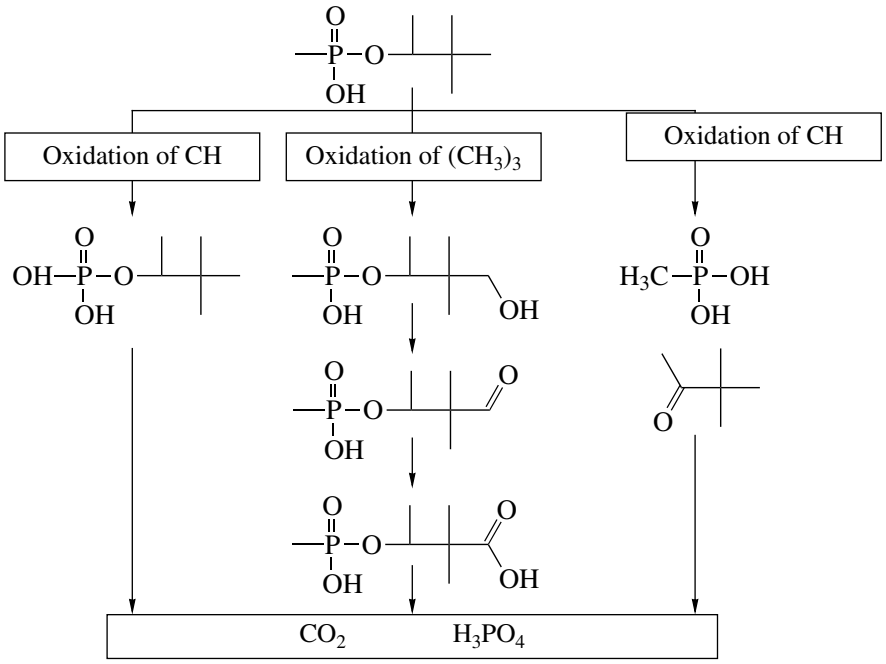

Fig. 14. Detected products and a conceivable scheme of the main initial reaction paths in the photocatalytic degradation of pinacolyl methylphosphonate in an aqueous suspension of Hombikat UV 100 TiO_2.

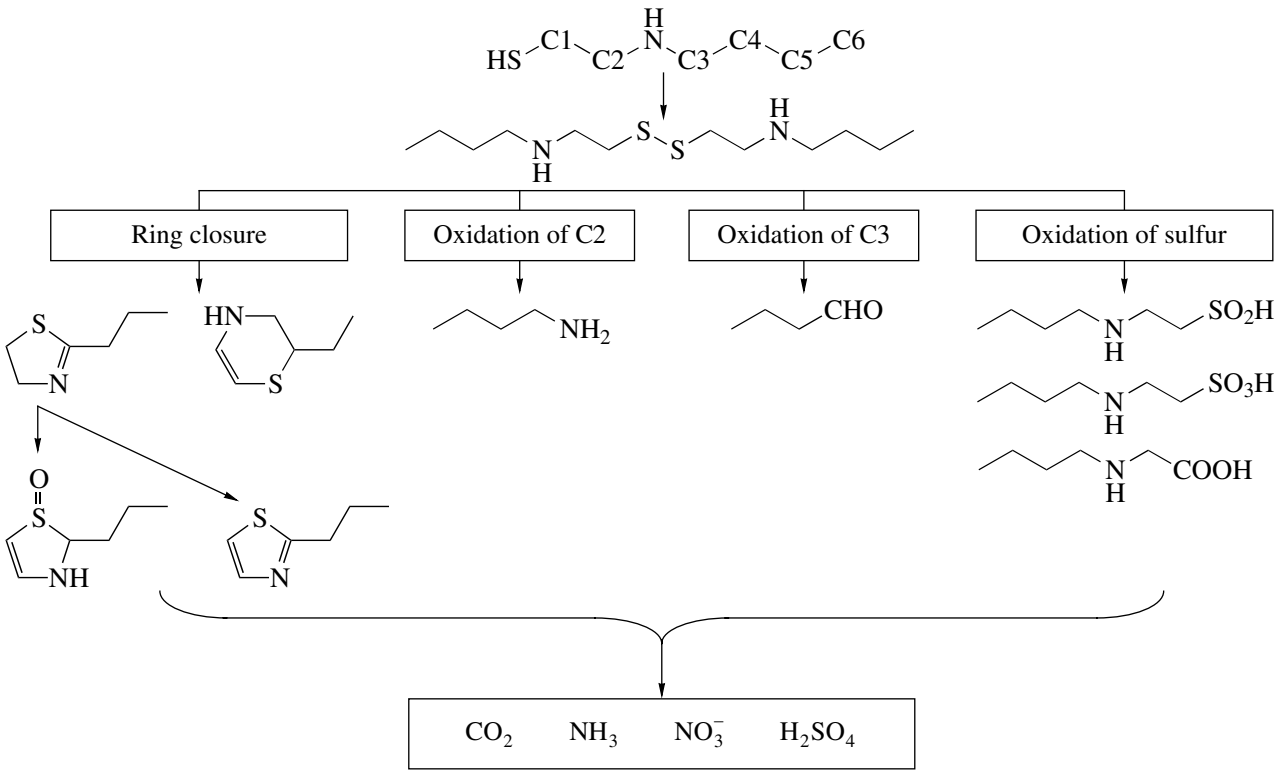

Fig. 15. Detected products and conceivable main reaction paths of the dark and photocatalytic reactions of 2-(butylamino)ethanethiol in the course of oxidation in an aqueous suspension of Hombikat UV 100 TiO_2.

the main reaction paths is the oxidation of the sulfur atom. In this case, it rapidly occurred in the absence of UV irradiation and led to a disulfide. The subsequent transformations were initiated by the photocatalyst under irradiation and involved ring closures, the oxidation of carbon atoms bound to the nitrogen atom, and a deeper oxidation of the sulfur atom in the disulfide. The introduction of a hydroxyl group into the simulant molecule at carbon atoms adjacent to the nitrogen atom resulted in the formation of aminols, which, as is well known, undergo hydrolysis to form corresponding amines and aldehydes. The oxidation of the disulfide sulfur atom led to a thiosulfonate, which undergoes hydrolysis with the formation of sulfinic acid. Next, this acid was oxidized to sulfonic and sulfuric acids. Finally, all of the reaction paths of 2-(butylamino)ethanethiol oxidation resulted in the formation of inorganic products: carbon dioxide, ammonia, sulfuric acid, and nitric acid.

CONCLUSIONS

Thus, we found that the photocatalytic activity of titanium dioxide can exhibit a maximum at a certain calcination temperature. In this case, the photocatalytic activity of samples calcined at various temperatures correlates with their whiteness (that is, the integral of diffuse-reflectance spectra).

Among photoreduced Pt/TiO_2 samples, a catalyst with platinum in a zero oxidation state exhibits the greatest activity in the photocatalytic oxidation of acetone vapor. The activity of Pt/TiO_2 samples prepared by the chemical reduction of H_2PtCl_6 is higher than that of the samples prepared by photocatalytic reduction. The enhanced activity of Pt/TiO_2, as compared with that of pure TiO_2, results from dark reactions and photoreactions on the surface of platinum, better charge separation, and greater adsorption of reactants.

The activity of TiO_2 in the photocatalytic oxidation reactions of acetone and benzene vapors increases after the treatment of the catalyst surface with sulfuric acid. In this case, a correlation between the activity and the number of acid sites on the surface of TiO_2 is observed. Moreover, an acceleration of photocatalytic oxidation on TiO_2 treated with the acid is accompanied by a decrease in the activation energy of the reaction and the facilitated desorption of CO_2, which is the final oxidation product.

The presence of a large amount of adsorbed reagents in a photocatalytic batch reactor significantly affects the kinetics of their consumption and can exert either a positive or negative effect on water and air purification.

The TiO_2 photocatalytic oxidation of sulfur-containing organic compounds can be accompanied by direct photolysis under exposure to soft UV light. In the photocatalytic oxidative degradation of the chemical

warfare agent simulants 2-phenethyl 2-chloroethyl sulfide, diethylphosphoramidate, pinacolyl methylphosphonate and 2-(butylamino)ethanethiol, many volatile and nonvolatile products are detected. In the photocatalytic oxidation of the last-named simulant, heterocyclic intermediate products are formed. The dark hydrolysis of intermediate products is an important step in the degradation of the simulants. Inorganic substances are the final products of the photocatalytic oxidation of the simulants.

The action of 20-kHz ultrasound on a suspension of TiO_2 did not cause the oxidation of dimethyl methylphosphonate dissolved in this suspension. However, it significantly accelerated the photocatalytic oxidation of this compound because of an accelerated transport of reactants to the surface of the photocatalyst.

ACKNOWLEDGMENTS

This work was supported by the Russian Foundation for Basic Research (project no. 02–03-08002) and the program "Leading Scientific Schools of Russia" (grant no. NSh 1484.2003.3). Vorontsov acknowledges the support of the Foundation for the Support of Domestic Science. This study was supported in part by the "Russia in Flux" program of the Academy of Finland (grant no. 208134).

REFERENCES

1. Kisch, H. and Lindner, W., *Chem. Unserer Zeit*, 2001, vol. 4, p. 250.
2. Coronado, J. M., Maira, A.J., Conesa, J.C., Yeung, K.L., Augugliaro, V., and Soria, J., *Langmuir*, 2001, vol. 17, p. 5368.
3. Vorontsov, A.V., Altynnikov, A.A., Savinov, E.N., and Kurkin, E.N., *J. Photochem. Photobiol., A*, 2001, vol. 144, nos. 2–3, p. 193.
4. Vorontsov, A.V., *Cand. Sci. (Chem.) Dissertation*, Novosibirsk: Catalysis Center, 1998.
5. Xi, C., Chen, Z., Li, Q., and Jin, Z., *J. Photochem. Photobiol., A*, 1995, vol. 87, p. 249.
6. Vorontsov, A.V., Savinov, E.N., and Jin, Z., *J. Photoch. Photobiol., A*, 1999, vol. 125, nos. 1–3, p. 113.
7. Vorontsov, A.V., Savinov, E.N., Barannik, G.B., Troitsky, V.N., and Parmon, V.N., *Catal. Today*, 1997, vol. 39, p. 207.
8. Vorontsov, A.V., Stoyanovz, I.V., Kozlov, D.V., Simagina, V.I., and Savinov, E.N., *J. Catal.*, 2000, vol. 189, p. 360.
9. Kennedy, J.C. and Datye, A.K., *J. Catal.*, 1998, vol. 179, p. 375.
10. Sun, B., Vorontsov, A.V., and Smirniotis, P.G., *Langmuir*, 2003, vol. 19, p. 3151.
11. Kozlov, D., Bavykin, D., and Savinov, E.N., *Catal. Lett.*, 2003, vol. 86, p. 169.
12. Kozlov, D.V., Panchenko, A.A., Bavykin, D.V., Savinov, E.N., and Smirniotis, P.G., *Russ. Chem. Bull.*, 2003, vol. 52, p. 1100.
13. Vorontsov, A.V. and Savinov, E.N., *Chem. Eng. J.*, 1998, vol. 70, no. 3, p. 231.
14. Vorontsov, A.V., Panchenko, A.A., Savinov, E.N., Lion, C., and Smirniotis, P.G., *Environ. Sci. Technol.*, 2002, vol. 36, no. 23, p. 5261.
15. Chen, Y.-C., Vorontsov, A.V., and Smirniotis, P.G., *Photochem. Photobiol. Sci.*, 2003, vol. 2, no. 6, p. 694.
16. Vorontsov, A.V., Davydov, L., Reddy, E.P., Lion, C., Savinov, E.N., and Smirniotis, P.G., *New J. Chem.*, 2002, vol. 26, no. 6, p. 732.